CLM - R 19

United Kingdom Atomic Energy Authority

RESEARCH GROUP

Report

NUMERICAL CALCULATIONS ON REVERSED FIELD HEATING IN THE THETATRON

G. B. F. NIBLETT
D. L. FISHER

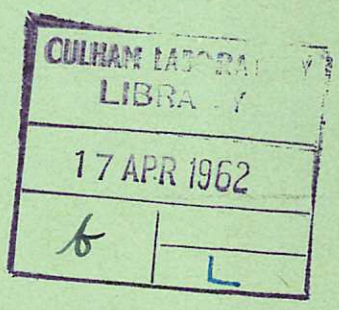

Culham Laboratory,

Culham, Abingdon, Berks.

1962

Available from H.M. Stationery Office
PRICE 4s. 0d. NET

U.D.C.
533 - 9
621 - 039 - 643

CLM - R 19

NUMERICAL CALCULATIONS ON REVERSED FIELD HEATING IN THE THETATRON

By

G. B. F. NIBLETT and D. L. FISHER

U. K. A. E. A. Research Group,
Culham Laboratory,
Abingdon,
Berks.

March, 1962
CR 62/152

NUMERICAL CALCULATIONS ON REVERSED FIELD HEATING IN THE THETATRON

G. B. F. Niblett
D. L. Fisher

Abstract

This report discusses numerical solutions of the two-fluid hydromagnetic equations designed to study the effect of trapped magnetic fields on the properties of a plasma compressed in the theta pinch. Conditions typical of the AWRE Maggi condenser banks are selected, i.e. deuterium at an initial pressure of 100 μ contained in a tube 4 cm in diameter is compressed by a field rising to 100 kilogauss in 2.5 μs. Initial bias fields of between + 5 and - 5 kilogauss are used and the effects of preheat and rate of compression are assessed. The calculations show that rapid joule heating is maintained by the large field gradients characteristic of reversed field discharges, and for an initial bias field of - 5 kg a peak electron temperature of 1.3 keV is predicted.

TABLE OF CONTENTS

1. INTRODUCTION

An important feature of magnetic compression experiments in θ pinch geometry is that the emission of soft X-rays and neutrons characteristic of a high temperature deuterium plasma occurs only in the presence of a trapped reversed magnetic field. This observation was first reported by Kolb, Dobbie and Griem [1] and has since been confirmed by numerous other research groups (see, for example, Refs. [2 - 4]). Experimentally the trapped field is produced by compression of a pre-ionized plasma permeated with an initial reversed bias field or by second half-cycle compression of a plasma containing remanent magnetic field from the first half-cycle.

Many explanations of the reversed field effect have been proposed, ranging from Kolb's original suggestion [1] which ascribed neutron production to the acceleration of deuterons by large E_θ fields generated by the interpenetration of the opposing magnetic fields, to the hypothesis [4] [5] that an imploding reversed field current sheath contained electrons of very high velocity which induced electrostatic instabilities accompanied by enhanced resistivity and magnetic field diffusion. However recent work has led to the recognition that the effect of reversed fields is probably twofold: firstly, there are the dynamic effects which result from closure of the reversed field lines round the plasma; and secondly there is rapid ohmic heating which originates from the large magnetic field gradient across the plasma. The dynamic effects associated with the closed field configuration predominate in short coils in which the plasma aspect ratio is small and are observed to engender an axial contraction which leads to instabilities [6] [7]. It seems likely that these dynamic processes are the source of the high ion temperatures which have been measured in short coils. The enhanced joule heating has been observed in long coils where it is divorced from the complicating axial motions, and has been clarified largely as a result of a set of numerical calculations on the fast θ pinch made by Kolb and Hain [8]. Their solution of the hydromagnetic equations using a programme compiled by Hain and Roberts [9] reveals a very rapid but otherwise classical joule heating process accompanying the interdiffusion of the reversed magnetic fields.

The present report summarises and discusses a set of numerical calculations similar to those of Kolb and Hain which have been expressly designed to study the heating effect of trapped reversed fields. The calculations are used to show the effect of bias fields and pre-ionization on the shock and joule heating processes when a driving field such as

that given by the Maggi banks at AWRE is used to compress a deuterium plasma. Pre-ionization temperatures of 5 eV and 3 eV are chosen, and the time scale of the compression is varied. The effect of thermal conductivity is considered briefly. The calculations confirm experimental observations [10] that the results of the compression depend mainly on the strength and sign of the trapped field. They also demonstrate that initial trapped fields of - 5 kg can produce electron temperatures greater than a kilovolt at peak compression.

2. THE HYDROMAGNETIC EQUATIONS

The numerical programme used for solving the hydromagnetic equations was a slightly modified version of that described by Hain and Roberts [9]. For the θ pinch the programme is simplified to include only B_z magnetic fields and E_θ electric fields. The programme treats a fully-ionized quasi-neutral plasma in which all variations are in the radial direction so that it cannot at present handle the initial partially-ionized phase, nor include the effects of axial contraction and expansion.* The plasma is assumed to be composed of separate electron and ion gases having maxwellian velocity distributions characterised by temperatures T_e and T_i and coupled by means of the usual relaxation equation for energy exchange. The electrons experience joule heating whereas shock heating is confined to the ions. No account is taken of loss of energy by radiation from the electron gas but separate ion and electron thermal conductivities across the magnetic field are incorporated.

The basic equations in the form in which they are used are as follows:-

Continuity Equation

$$\frac{\partial n}{\partial t} + \frac{1}{r}\frac{\partial}{\partial r}(rnv) = 0,$$

where $n = n_e = n_i$ is the particle density, r is the radial co-ordinate and v is the radial velocity.

---

* Numerical programmes which include partial ionization effects and longitudinal contraction and expansion are currently being prepared at AERE, Harwell by Dr. K. V. Roberts and his colleagues.

Momentum Equation

$$nm\left(\frac{\partial v}{\partial t} + v\frac{\partial v}{\partial r}\right) = -\frac{\partial}{\partial r}\left(nkT_e + nkT_i\right) - \frac{\partial q_i}{\partial r} - \frac{\partial}{\partial r}\left(B_Z^2/8\pi\right),$$

where m is the atomic mass, k is Boltzman's constant and q_i is the von Neumann viscous pressure used for treating shocks. The use of this von Neumann term for artifically broadening shock fronts is discussed by Richtmeyer [11].

Electron Temperature Equation

$$\frac{\partial(kT_e)}{\partial t} + \frac{v\partial(kT_e)}{\partial r} = -(\gamma - 1)kT_e\,\frac{1}{r}\,\frac{\partial}{\partial r}(rv) + \frac{(\gamma - 1)}{n}\,\frac{1}{r}\,\frac{\partial}{\partial r}\left(\varkappa_e r\,\frac{\partial T_e}{\partial r}\right)$$

$$+ \frac{(\gamma - 1)}{n}\,\eta j_\theta^2 - \frac{(kT_e - kT_i)}{t_{eq}},$$

where $\varkappa_e$ is the electron thermal conductivity, $j_\theta = -\frac{1}{4\pi}\frac{\partial B_Z}{\partial r}$ is the current, η is the electrical resistivity and t_{eq} is the ion-electron relaxation time.

Ion Temperature Equation

$$\frac{\partial(kT_i)}{\partial t} + \frac{v\partial(kT_i)}{\partial r} = -(\gamma - 1)\left(kT_e + \frac{q_i}{n}\right)\frac{1}{r}\,\frac{\partial}{dr}(rv)$$

$$+ \frac{(\gamma - 1)}{n}\,\frac{1}{r}\,\frac{\partial}{dr}\left(\varkappa_i r\,\frac{\partial T_i}{\partial r}\right) + \frac{(kT_e - kT_i)}{t_{eq}},$$

where $\varkappa_i$ is the ion thermal conductivity.

B_Z Field Equation

$$\frac{\partial B_Z}{\partial t} + \frac{v\partial B_Z}{\partial r} = -B_Z\,\frac{1}{r}\,\frac{\partial}{\partial r}\,(rv) + \frac{1}{r}\,\frac{\partial}{\partial r}\left(\frac{\eta r}{4\pi}\,\frac{\partial B_Z}{\partial r}\right).$$

Since collision times are much less than compression and oscillation times the electron and ion gases behave three-dimensionally so that

the specific heat ratio γ can be put equal to $\frac{5}{3}$.* Numerical values for the coefficients used in the calculations are defined in the Appendix. However, it is important to note here that in a strong field the thermal conduction coefficients vary inversely as the product $\omega^2\tau^2$, where ω is the Larmor frequency and τ the collision time. Since ω is much less for the ions than for the electrons because of the larger ion Larmor radius, the ion thermal conductivity is much greater than the electron thermal conductivity.

The detailed numerical methods of solving the equations have been described by Hain [12]. The boundary conditions used were essentially the same as those described in Ref. [9] except that the circuit details were eliminated and the external field B prescribed to be a sinusoid of the form

$$B = B_{max} \sin(\Omega t - \delta),$$

where B_{max} was 100 kg and Ω was chosen to give a quarter period of either 2.5 μs or 12.5 μs. The quantity δ was adjusted to ensure that at the beginning of the calculation the driving field was of the same sign and amplitude as the trapped field. Other conditions were as follows:-

Tube radius r_o:	2.0 cm
Initial deuterium pressure p_o:	100 μ
Line density N:	8.9×10^{16} cm^{-1}
Line mass Nm_i:	3.0×10^{-7} g/cm
Initial trapped field B_T:	+ 5, + 2, + 1, 0, - 0.1, - 1, - 2, - 5 kg
Initial ion and electron temperature:	5 eV and 3 eV

* The programme is at present being modified to include separate ion temperatures in the perpendicular and parallel directions in order to study the effect of very rapid oscillations on ion heating.

The hydromagnetic equations were solved on the AWRE IBM 7090 computer using these initial conditions.

At the beginning of a run the magnetic field just within the plasma must be set equal to the value in the insulating wall (for otherwise there would be a surface current), so that during the reversed field runs the plasma moves outwards initially because the external magnetic pressure first decreases to zero before rising to its peak value. Such an accumulation of plasma at the wall is observed experimentally. This process coupled with the boundary conditions (which require the removal and creation of plasma at the wall as the field lines leave and re-enter) led to numerical difficulties at high values of initial reversed fields of which the symptoms were a loss of plasma particles. Because of this difficulty the calculations were limited to trapped fields of up to 5 kg.

3. NUMERICAL RESULTS AND DISCUSSION

3.1 Commentary on the Graphs

The following plasma properties were computed as a function of radius throughout the first quarter-cycle of the discharge: velocity V, particle density n, electron temperature T_e, ion temperature T_i, magnetic field B_Z, current density j_θ, and ratio of plasma pressure to external magnetic pressure β. Graphs showing variations of some of these parameters across the tube at various times are shown in Figures 1 to 6 for initial trapped fields B_T of + 2 and - 2 kg. These values of B_T were selected in order to compare the effect of parallel and reversed trapped field.

Figures 1 and 2 show an early stage of the implosion just after the plasma has left the wall. In the reversed field discharge the density exhibits a sharp peak at the neutral surface which is also commonly observed in streak and framing camera photographs. The electron temperature is markedly higher in the reversed field configuration. As a consequence of field diffusion and hydromagnetic flow the magnetic pressure and particle density ahead of the sheath have increased with parallel B_T whereas they have decreased with negative B_T. These differing results of field diffusion explain the greater implosion velocities observed with reversed fields.

A later stage of the implosion is shown in Figures 3 and 4. The sharp density peak at the neutral surface typical of reversed B_T is again apparent as is the much greater field gradient in the reversed configuration. The rate of joule heating per unit volume is given by j^2_θ/σ, where σ is the conductivity so that the source of the high electron temperatures of Figure 4 is evidently the high current densities. Both Figures 3 and 4 show a large increase in electron temperature in the plasma sheath where the density is low, but this feature is particularly marked in Figure 4.

Figures 5 and 6 present conditions at peak field. The reversed field discharge has a high electron temperature rising to 460 eV where the density is a maximum. The plasma is concentrated in an annulus with an inner core of trapped field. This central hollow core is a characteristic of reversed field configurations which is observed experimentally [4] [10]. The plasma radius is similar in both figures so that the mean plasma densities are approximately the same. For parallel B_T the ion and electron temperatures are tied closely together; this is partly a consequence of the rapid energy exchange at low temperatures and partly a result of similar rates of shock and joule heating. The remarkably uniform ion temperature in Figures 5 and 6 is a result of the high thermal conductivity of the ion gas. The higher the temperature the more uniform the temperature distribution (compare previous figures) since the thermal conductivity increases as $T^{5/2}$.

Figure 7 presents the variation of trapped reversed flux for various values of B_T and shows that most of the flux dissipation occurs during the implosion. It is convenient to separate the first quarter-cycle into two stages, the dynamic stage which consists of the implosion and subsequent plasma bouncing and lasts approximately 0.5 μs (2.5 μs for a quarter period of 12.5 μs), and the compression stage which is the remainder of the quarter cycle until peak current. Most of the flux dissipation takes place during the dynamic phase in agreement with the conclusions reached experimentally by Little et al [4] and Reynolds and Phillips [12]. During the compression stage the decay of trapped flux is relatively slow; however the heating produced by flux dissipation is greater when the field is high since the magnetic energy is proportional to the square of the field strength. Some trapped flux remains for the complete quarter-cycle except with

B_T of - 0.1 kg when it is completely dissipated after 1.36 μs.

The dissipation of trapped flux for the discharge with 12.5 μs quarter period is shown in Figure 8 for B_T of - 2 kg. The conclusions are much the same as for the more rapid discharge: the trapped flux disappears in the early stages and is completely gone by 9 μs.

3.2 Tabulated Results

In Table 1 the computed values of n, T_e, T_i, β , j_θ and V at the end of the dynamic phase (0.5 μs) and the end of the compression phase (2.5 μs) are tabulated to show the effect of initial trapped field. In compiling the table maximum values of the various quantities have been chosen; the values of T_e and T_i are those which correspond to peak density rather than the higher values in the sheath. Similarly the current densities quoted are for the main bulk of plasma rather than the boundary values.

The table shows that the peak implosion velocity is constant over most of the range of B_T, but falls off for large positive values and increases for large negative values. For B_T of + 5 kg the implosion is slowed down by compression of the parallel field ahead of the plasma, whereas in the reversed field discharge the rapid diffusion and cancellation of field lowers the magnetic pressure ahead of the wave. This rapid diffusion is accompanied by an electric field in the plasma whose direction is such as to increase the rate of flow of electromagnetic energy into the system, i.e., the effect is to suck the plasma into the centre.

Table 1 displays the increase in current density as the initial field goes from + 5 kg to - 5 kg. The high current densities support the high field gradients in the neighbourhood of the neutral surface. Thus the programme supports the conclusions of Kolb and Hain [8] that the principal effect of reversed fields is to heat the electrons by a resistive mechanism. For example, for B_T of - 5 kg the electron temperature at the end of the dynamic phase is 460 eV rising to 1310 eV at the end of the compression. Despite the high current densities the calculations show that at all points in the plasma the electron drift velocities are subsonic so that there is no reason to suppose that the reversed field sheath suffers from electrostatic instabilities. In addition to supplying a powerful electron heating

mechanism the trapped reversed field maintains a high β. In the neutral surface the plasma β is necessarily unity and the computations show that throughout the plasma the average β is greater than 0.5.

The computed values of T_e and T_i at the end of the dynamic phase allow a rough estimate of the relative importance of shock heating and joule heating in discharges with differing B_T. In strong parallel fields the ions are hotter than the electrons at this stage disclosing that the ions are being heated by shock heating more rapidly than the electrons are being heated by joule effects; the ions are therefore dragging the electron temperature upwards. With large negative B_T the joule heating is more rapid than shock heating (even though the implosion velocity has increased) and the electron temperature drags the ion temperature upwards. In the parallel field discharges the electron and ion temperatures are the same at peak field whereas in reversed fields the electron temperature is much higher. Indeed for B_T of - 5 kg the ion temperature is lower than when B_T is - 2 kg because the higher electron temperatures have reduced the energy exchange rate. The highest ion temperature achieved by peak field is 350 eV; this strongly suggests that the high ion temperatures and neutron emission observed in short coils are a result of the dynamic axial motions produced by reversed fields and not a result of purely radial motion. It should be noted that the programme does not include the effect of radiation losses on the cooling of the electrons; this will be important if the discharge contain high Z impurities.

A conclusion which can be drawn from Table 1 is that the plasma conditions at the end of the compression phase correspond approximately to isentropic compression of the plasma produced at the end of the dynamic phase. This applies with particular force to the plasma density and electron temperature. Thus in general it can be said that the dynamic phase is irreversible, whereas the compression phase is reversible. This statement is not strictly true since there is a continual irreversible exchange of energy between the ions and electrons as they relax towards a common temperature, but it is an approximation sufficiently good for many purposes.

The plasma properties in the slower discharge with quarter period 12.5 μs are tabulated in Table 2 for B_T of + 2 kg and - 2 kg. They show the effect of speed of compression on the heating mechanisms. The implosion velocities are low and there is virtually

no shock heating so that even in the parallel field discharge the electrons are hotter than the ions at the end of the dynamic phase. Because of the lower temperatures and longer times the ion and electron temperatures are closely matched. The effect of the reversed field heating is considerable, since the particles reach a temperature of over 400 eV by peak field.

3.3 Effect of Pre-Ionization and Thermal Conductivity

In order to assess the effect of pre-ionization temperature the computations with B_o of $\pm$ 2 kg were repeated with initial plasma temperatures of 3 eV. Temperatures lower than this were not used since an equilibrium plasma would not then be fully ionized. It was found that varying the initial temperature had a much smaller effect on the subsequent discharge than variations in trapped field. This result was taken as confirming the conclusion put forward in Ref. [10] that it is the initial trapped field which predominantly determines the subsequent development.

The calculations with B_o of $\pm$ 2 kg were also repeated with the heat conduction coefficients put equal to zero. The results verified the importance of thermal conductivity particularly in smoothing out the ion temperatures. The tendency is for joule heating to take place mainly in the neutral surface and at the plasma boundary, whereas the ion heating is greatest on the axis where the shocks are reflected. Thermal conductivity plays an essential role in conducting heat away from these regions. For example without thermal conduction and for reversed B_T of 2 kg the ion temperature rose to 10 keV on the axis and the steepness of the temperature gradients eventually led to breakdown of the programme.

4. CONCLUSION

These numerical calculations confirm the predominant effect of trapped field in determining the plasma temperatures produced by rapid compression in axial magnetic field experiments. Compression of an initial trapped field of - 5 kg by an external field rising to 100 kg in 2.5 μs results in electron temperatures of 1.3 keV and particle densities of 1.5×10^{17} cm^{-3}. An additional feature of the trapped reversed field is that it maintains a high average β in the plasma. The mechanism responsible for the high temperature is ohmic heating whose rate is particularly rapid because of the high field gradients which are

sustained by the reversed field configuration. Despite the high current densities the electrons remain subsonic. The calculations show that the effect of the trapped reversed field is much greater than the effect of the preheat temperature, and that transport of energy by thermal conduction is an important means of smoothing the temperature gradients.

In the fast discharges considered the shock heating gives ion temperatures of approximately 100 eV, but in the presence of trapped reversed fields this is obscured by the more rapid joule heating. Calculations at lower rates of rise verify that though shock heating is much reduced the reversed field heating is less sensitive to the rate of compression. Thus an advantage of reversed field heating is that it does not require rapid compression rates and for this reason it is likely to become an important means of heating a dense plasma to kilovolt temperatures.

5. ACKNOWLEDGMENTS

The authors wish to acknowledge their indebtedness to Dr. K. V. Roberts for many valuable suggestions and much helpful encouragement during the course of the calculations.

APPENDIX

COEFFICIENTS USED IN THE CALCULATIONS

The numerical values given here are those adopted by Roberts [14]. The electrical resistivity is taken to be the value appropriate to a strong transverse magnetic field [15].

$$\eta = \frac{\pi^{3/2} m_e^{1/2} e^2 c^2 \log \Lambda}{2(2kT_e)^{3/2}.(0.582)},$$

where [15]

$$\Lambda = \frac{3}{2e^3} \frac{(kT_e)^{3/2}}{(\pi r)^{1/2}}.$$

The relaxation time between electrons and ions is [15]

$$t_{eq} = \frac{3mm_e(kT_e/m_e)^{3/2}}{8(2\pi)^{1/2} ne^4 \log \Lambda}.$$

The thermal conductivities are written in the form

$$\varkappa = \frac{A\tau}{1 + B\omega^2\tau^2},$$

where A and B are chosen so that $\varkappa$ is correct in the limit of both strong and weak magnetic fields. At the time when the coefficients were worked out, it was noticed that the total plasma thermal conductivity given by Marshall [16] was incorrect, since it evidently allowed only for transport of heat by electrons. His value was in fact used to determine the strong field thermal conductivity for electrons

$$\varkappa_{es} = \frac{2kn\tau_e(kT_e)}{m_e} \frac{6.79}{\omega_e^2\tau_e^2},$$

where

$$|\omega_e| = eB/m_eC$$

and

$$\tau_e = \frac{3}{\sqrt{2\pi}} \frac{m_e^{1/2}(kT_e)^{3/2}}{2ne^4\psi},$$

(The quantity n used by Marshall is equal to the total number of particles (ions and electrons), but this has been allowed for in quoting his expressions.) It is assumed that $\psi = 2 \log \Omega$. The weak-field electron thermal conductivity is taken from Spitzen [15]

$$\varkappa_{eo} = 20\left(\frac{2}{\pi}\right)^{3/2} \frac{(kT_e)^{5/2}}{m_e^{1/2}e^4 \log \Lambda} k \cdot (0.419)(0.225).$$

The strong-field ion thermal conductivity is taken from Rosenbluth and Kaufmann [17]

$$\varkappa_{is} = \left(\frac{2m}{m_e}\right)^{1/2} \frac{(kT_i)k}{B^2} \eta^*,$$

where $\eta^*(T_i) = \eta(T_e)$. (The previous remarks about η apply here also). The weak-field value is taken from Marshall [18]

$$\varkappa_{io} = 1.08 \frac{75}{16\sqrt{\pi}} \frac{k(kT_i)^{5/2}}{m_i^{1/2}e^4\psi}.$$

Thermoelectric effects are neglected.

The source of the error in Ref. [16] was subsequently found by Vaughan-Williams and Haas [19].

REFERENCES

1. A. C. Kolb, C. B. Dobbie and H. R. Griem: "Field Mixing and Associated Neutron Production in a Plasma". Phys. Rev. Letters, 3, 5, (1959).

2. H. Fay, E. Hintz and H. L. Jordan: "Experiments on Shock Compression of Plasmas". Proc. of the 4th Int. Conf. on Ionization Phenomena in Gases, Uppsala, 1046 (1959).

3. H. A. B. Bodin et al: "An Experimental Investigation of the Rapid Compression of a Plasma Using Azimuthal Currents (Thetatron)". Proc. of the 4th Int. Conf. on Ionization Phenomena in Gases, Uppsala, 1061 (1961).

4. E. M. Little, W. E. Quinn and F. L. Ribe: "Effects of Ionization and Magnetic Initial Conditions on a Magnetically Compressed Plasma (Scylla)". Physics of Fluids, 4, 711 (1961).

5. R. C. Mjolsness, F. L. Ribe and W. B. Riesenfield: "Self-Consistent Reversed Field Sheath". Physics of Fluids, 4, 730 (1961).

6. M. Dazey, V. Josephson and R. Wuerker: "Instability Mechanisms in Transverse Pinches". Phys. Rev. Letters, 5, 416 (1960).

7. H. A. B. Bodin et al.: "Rapid Axial Contraction of a High Density Deuterium Plasma in a Thetatron Discharge". Salzburg Conference on Nuclear Fusion (1961).

8. K. Hain and A. C. Kolb: "Fast Theta Pinch", Salzburg Conference on Nuclear Fusion (1961).

9. K. Hain, K. V. Roberts et al.: "Fully Ionized Pinch Collapse". Zeitschrift fur Naturforschung, 15a, 1039 (1960).

10. H. A. B. Bodin et al.: "The Influence of Trapped Field on the Characteristics of a Magnetically Compressed Plasma (Thetatron)". Salzburg Conference on Nuclear Fusion (1961).

11. R. D. Richtmeyer: "Difference Methods for Initial-Value Problems". Interscience, New York (1957).

REFERENCES (CONT.)

12. K. Hain: AERE Report No. R3383 (1961).

13. J. A. Reynolds and N. J. Phillips: "Magnetic Field Diffusion during the Initial Stages of the Theta Pinch". Proc. of the 5th Int. Conf. on Ionization Phenomena in Gases, Munich (1961).

14. K. V. Roberts: Private Communication (1960).

15. L. Spitzer Jr.: "Physics of a Fully Ionized Gas". Interscience New York (1956).

16. W. Marshall: "Kinetic Theory of an Ionized Gas, Part 3". AERE Report No. T/R2419 (Unpublished) (1958).

17. M. Rosenbluth and A. Kaufmann: Phys. Rev., 109, 1 (1958).

18. W. Marshall: "Kinetic Theory of an Ionized Gas, Part 1", AERE Report No. T/R2247 (Unpublished) (1958).

19. R. W. Vaughan-Williams and F. A. Haas: Phys. Rev. Letters, 6, 165 (1961).

TABLE 1

Numerical Calculations of Reversed Field Heating in the Thetatron

The driving magnetic field is a sine wave which rises to a peak of 100 kilogauss in 2.5 μs.
The calculations are for deuterium gas in a tube 4 cm in diameter.
Initial conditions: $n_i = n_e = n = 7.1 \times 10^{15}$ cm^{-3}

$T_e = T_i = 5$ eV.

Initial Trapped Field B_T, kilogauss	Peak Implosion Velocity V cm/μs	Conditions after 0.5 μs External Field 30 kg					Conditions after 2.5 μs External Field 100 kg				
		n_{max}, cm^{-3}	$T_{e_{max}}$†, eV	$T_{i_{max}}$†, eV	β_{max}	$j_{\theta_{max}}$, kA/cm^2	n_{max}, cm^{-3}	$T_{e_{max}}$, eV	$T_{i_{max}}$, eV	β_{max}	$j_{\theta_{max}}$, kA/cm^2
+ 5.0	9.0	3.8×10^{16}	58	135	0.18	33	1.4×10^{17}	115	115	0.10	30
+ 2.0	12.7	7.3×10^{16}	93	200	0.56	50	2.4×10^{17}	150	140	0.30	110
+ 1.0	12.6	9.5×10^{16}	117	180	0.88	100	3.7×10^{17}	220	200	0.53	200
0.0	12.5	1.1×10^{17}	115	120	1.00	145	4.5×10^{17}	320	270	0.95	400
- 0.1	12.3	1.2×10^{17}	120	140	1.00	160	4.5×10^{17}	340	270	0.98*	480
- 1.0	12.2	1.1×10^{17}	130	145	1.00	260	3.6×10^{17}	400	330	1.00	650
- 2.0	12.6	1.0×10^{17}	200	118	1.00	400	3.1×10^{17}	470	350	1.00	900
- 5.0	15.3	5.1×10^{16}	460	260	1.00	900	1.5×10^{17}	1310	250	1.00	2400

*Reversed field completely dissipated after 1.36 μs.

†Approximate values only, since there are rapid variations in T_e and T_i during the early stages.

TABLE 2

Numerical Calculations of Reversed Field Heating in the Thetatron

The driving magnetic field is a sine wave which rises to a peak of 100 kilogauss in 12.5 μs
The calculations are for deuterium gas in a tube 4 cm in diameter.
Initial conditions: $n_i = n_e = n = 7.1 \times 10^{15}$ cm^{-3}

$$T_e = T_i = 5 \text{ eV}$$

Initial Trapped Field B_T, kilogauss	Peak Implosion Velocity V cm/μs	Conditions after 2.5 μs External Field 30 kg					Conditions after 12.5 μs External Field 100 kg				
		n_{max}, cm^{-3}	$T_{e_{max}}$†, eV	$T_{i_{max}}$†, eV	β_{max}	$j_{\theta_{max}}$, kA/cm^2	n_{max}, cm^{-3}	$T_{e_{max}}$, eV	$T_{i_{max}}$, eV	β_{max}	$j_{\theta_{max}}$, kA/cm^2
+ 2	3.5	9.2×10^{16}	48	41	0.23	20	2.4×10^{17}	114	86	0.14	45
- 2	5.0	9.5×10^{16}	160	120	1.00	140	2.9×10^{17}	470	415	0.96*	400

*Reversed field completely dissipated after 9 μs.

†Approximate values only, since there are rapid variations in T_e and T_i during the early stages.

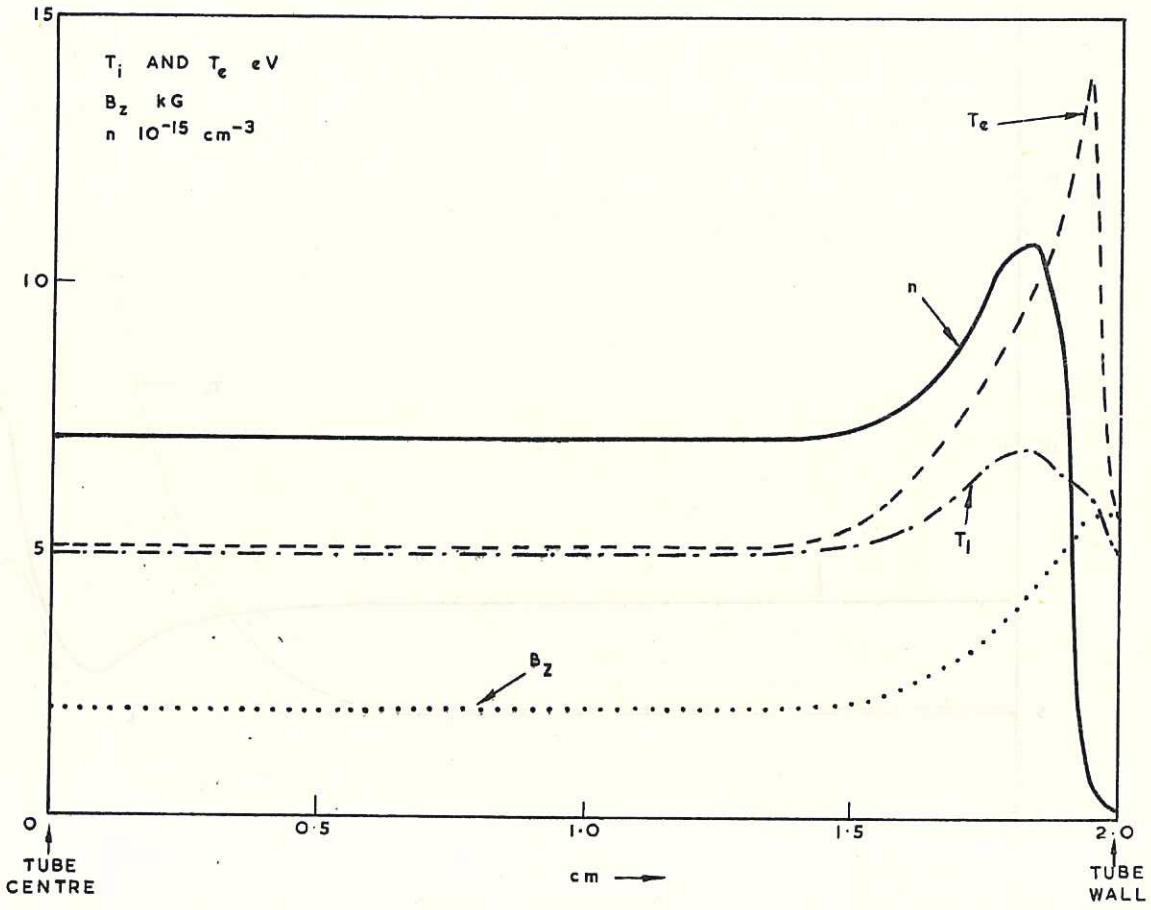

FIGURE I. PLASMA CONDITIONS AT AN EARLY STAGE OF THE IMPLOSION. INITIAL TRAPPED MAGNETIC FIELD + 2 kG. TIME 0·092 μs.

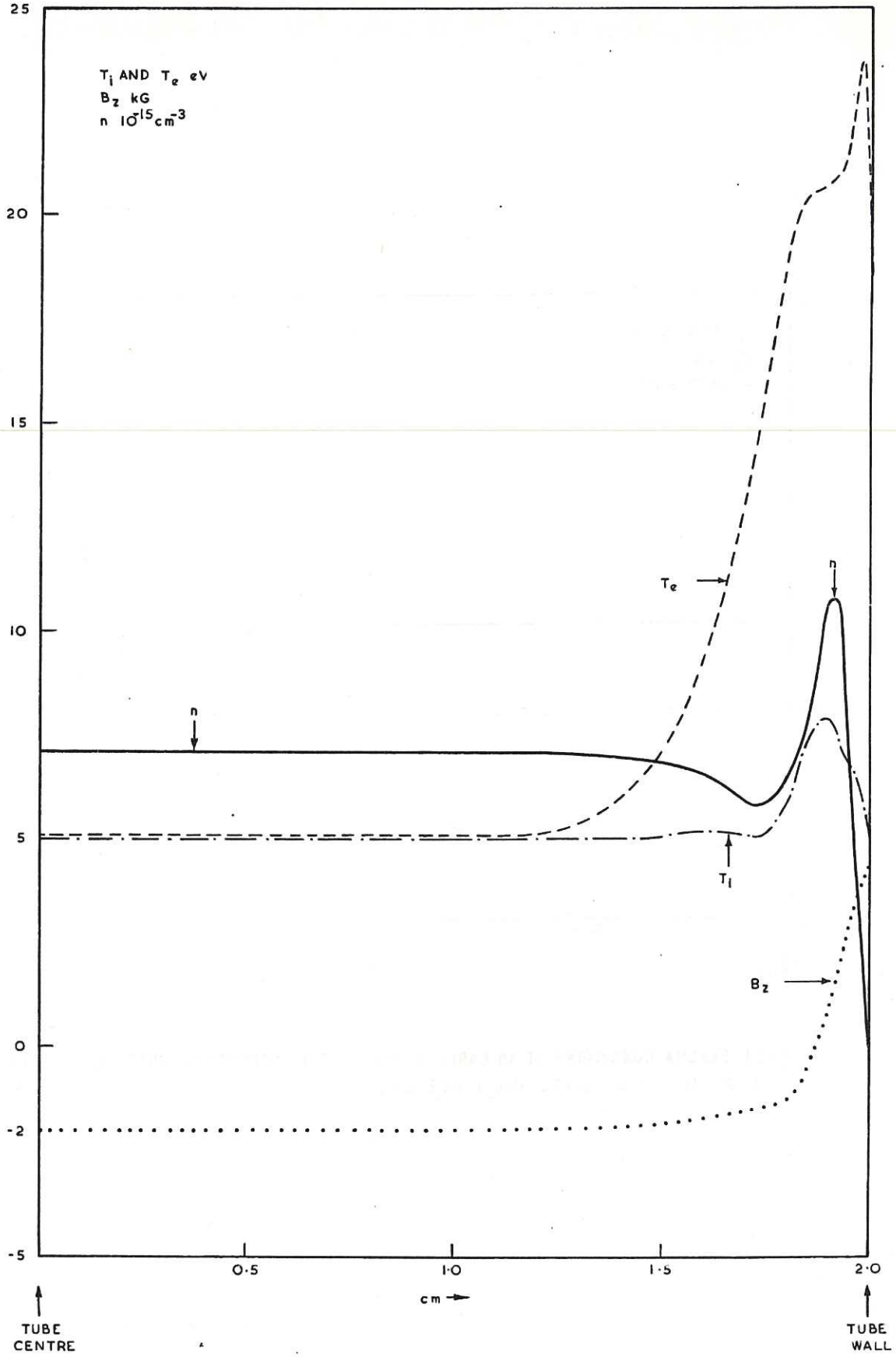

FIGURE 2. PLASMA CONDITIONS AT AN EARLY STAGE OF THE IMPLOSION. INITIAL TRAPPED MAGNETIC FIELD – 2 kG. TIME 0·069 μs.

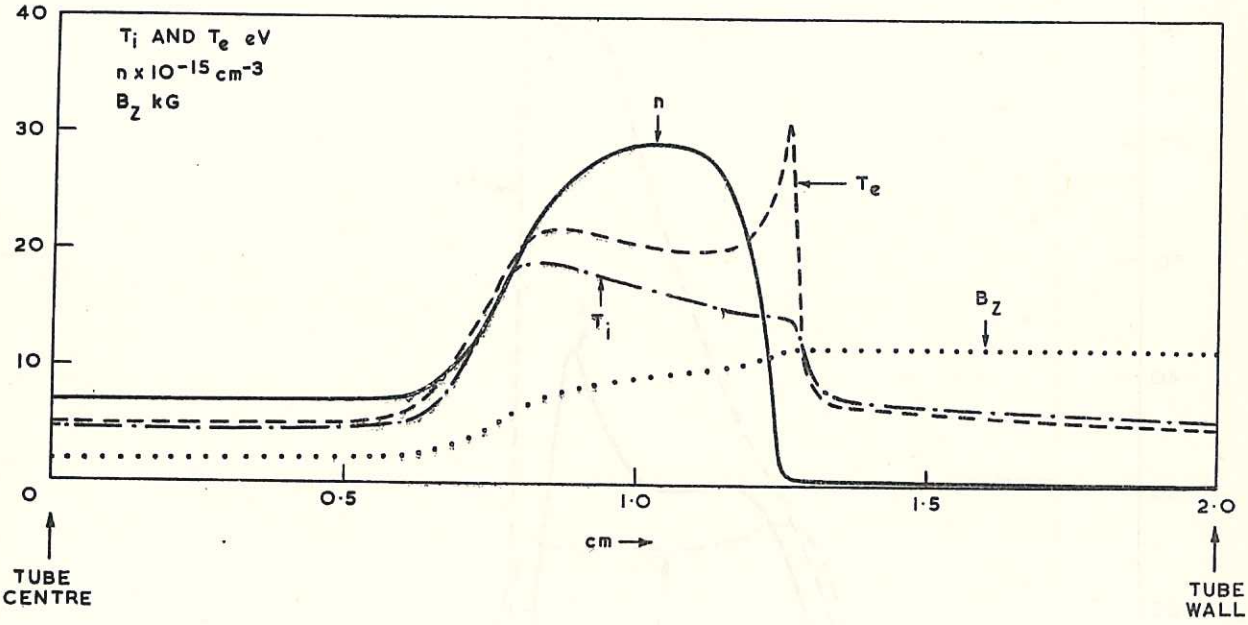

FIGURE 3. PLASMA CONDITIONS AT A LATER STAGE OF THE IMPLOSION. INITIAL TRAPPED MAGNETIC FIELD + 2 kG. TIME 0·188 μs.

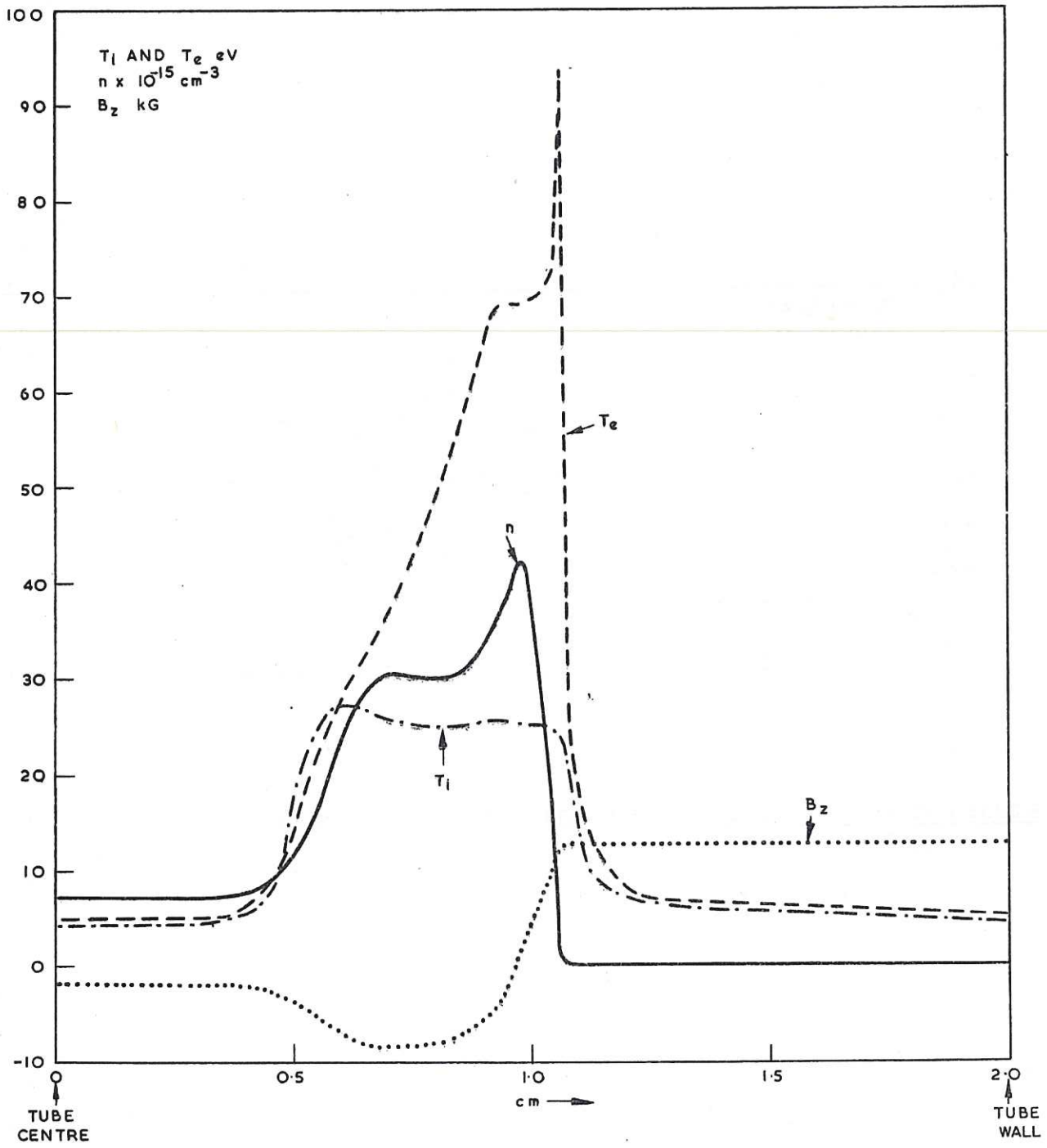

FIGURE 4. PLASMA CONDITIONS AT A LATER STAGE OF THE IMPLOSION. INITIAL TRAPPED MAGNETIC FIELD - 2kG. TIME 0·201 μs.

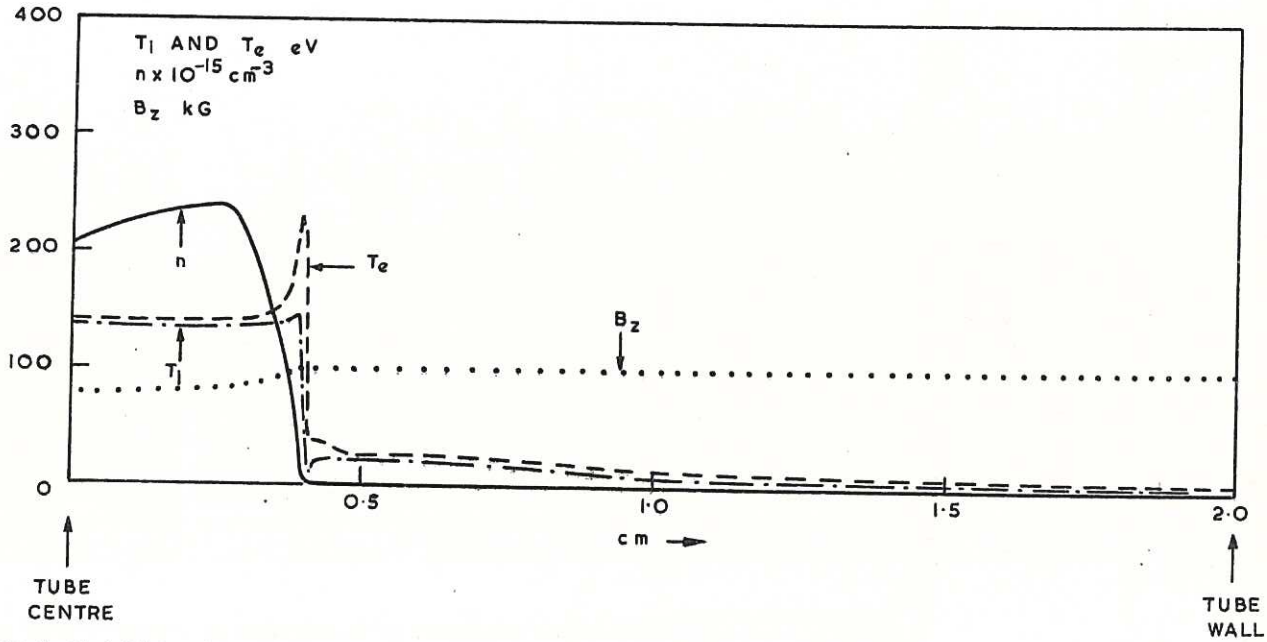

FIGURE 5. PLASMA CONDITIONS AT PEAK FIELD. TRAPPED MAGNETIC FIELD + 2 kG. TIME 2·5 μs.

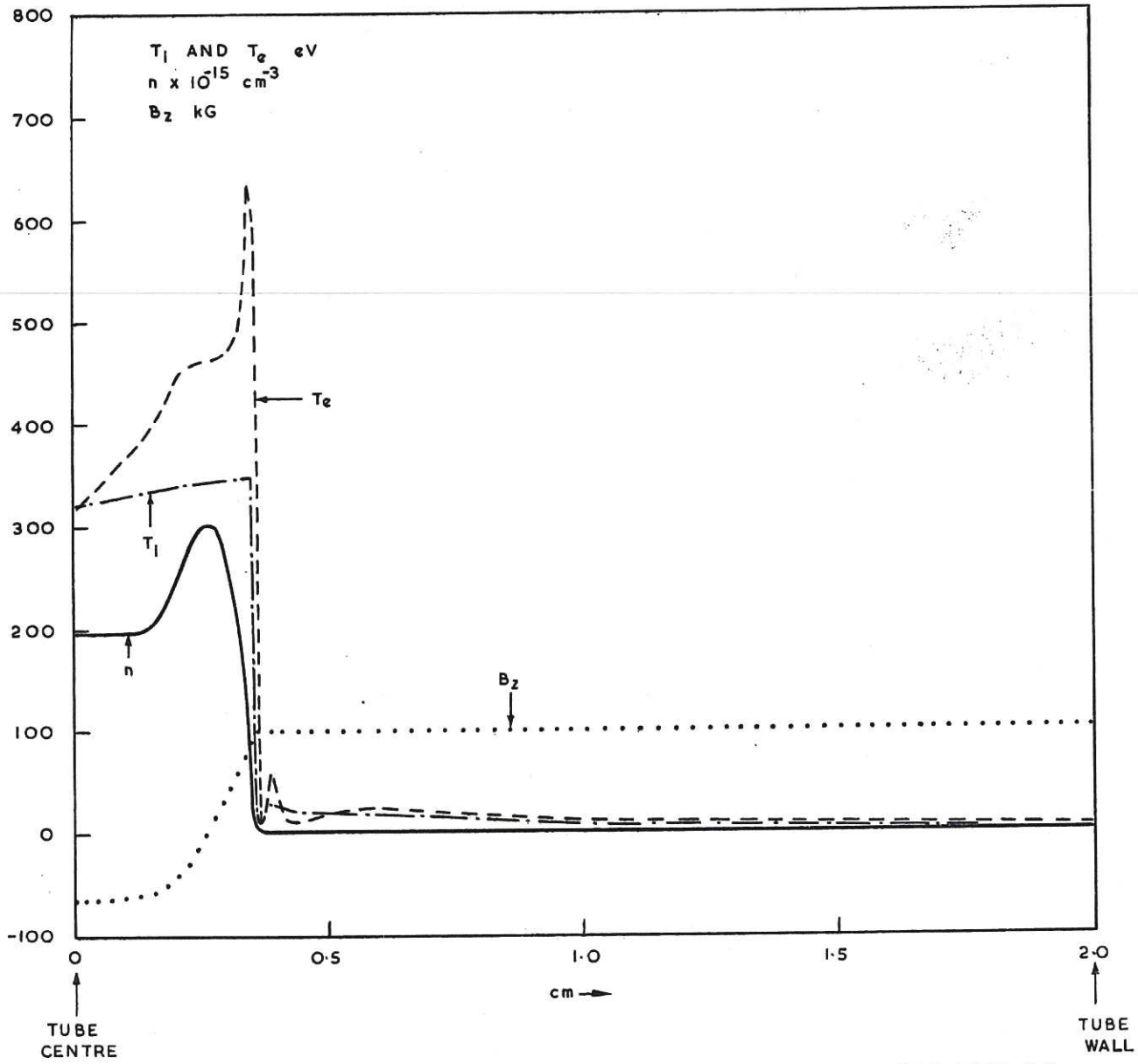

FIGURE 6. PLASMA CONDITIONS AT PEAK FIELD. TRAPPED MAGNETIC FIELD 2 kG. TIME 2·5 μs.

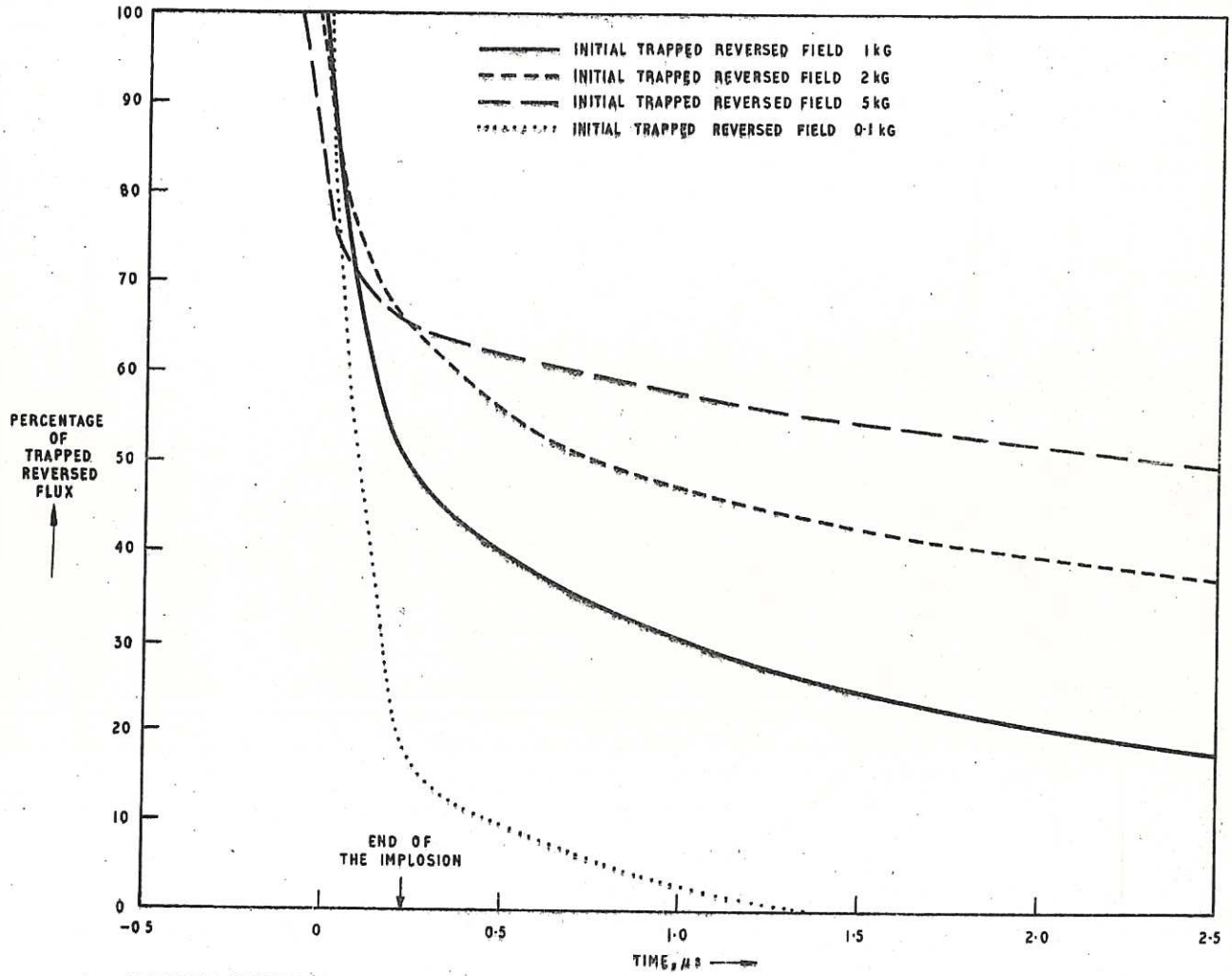

FIGURE 7. DECREASE IN TRAPPED REVERSE FLUX AS A FUNCTION OF TIME FOR THREE VALUES OF INITIAL TRAPPED REVERSED FIELD. THE EXTERNAL MAGNETIC FIELD RISES TO 100 kG IN 2·5 μs

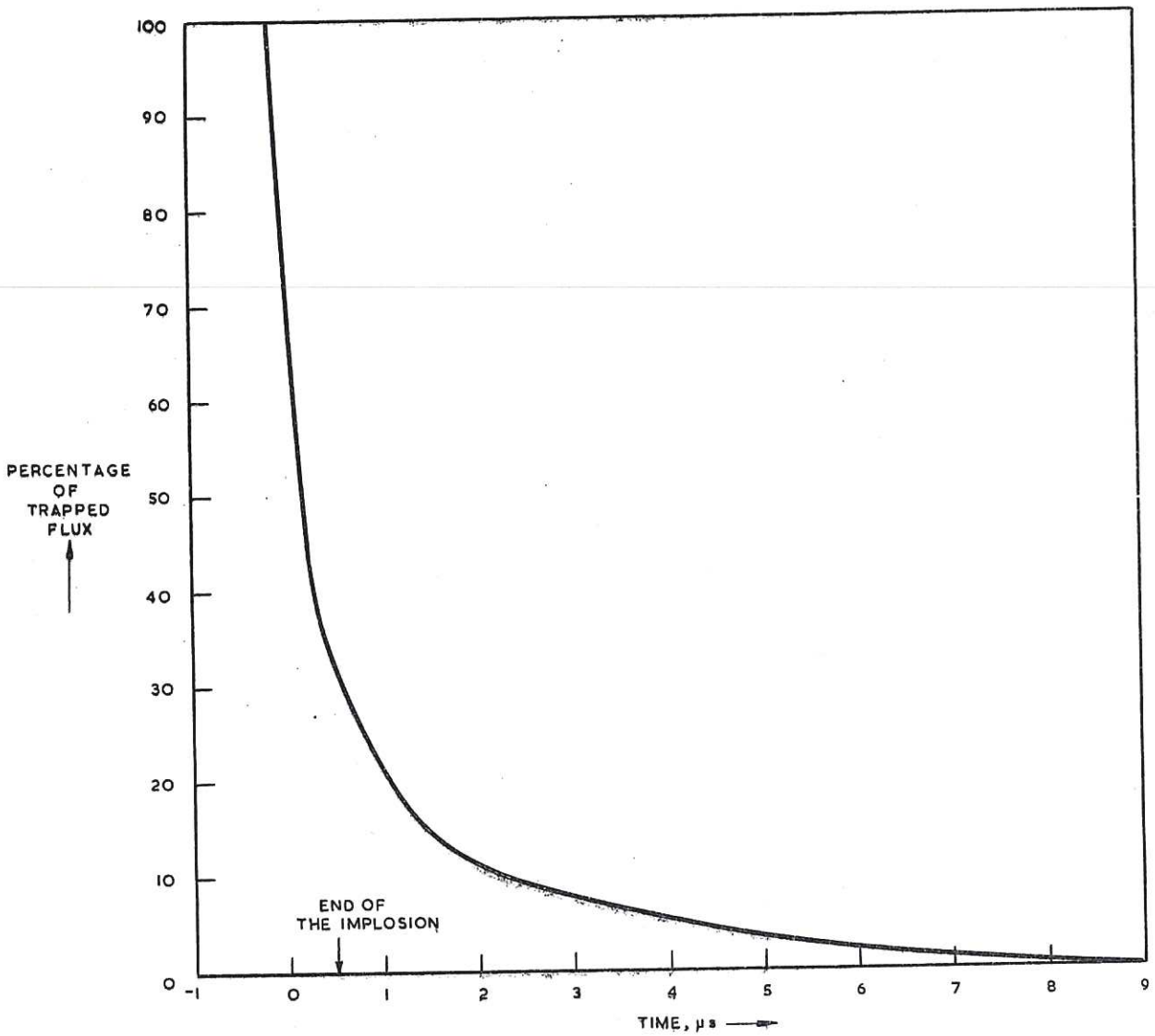

FIGURE 8. DECREASE IN TRAPPED REVERSE FLUX AS A FUNCTION OF TIME FOR A DISCHARGE IN WHICH THE DRIVING FIELD RISES TO 100 kG IN 12·5 μs. THE INITIAL TRAPPED FIELD WAS - 2 kG

Available from

HER MAJESTY'S STATIONERY OFFICE

York House, Kingsway, London W.C. 2

423 Oxford Street, London W. 1

13a Castle Street, Edinburgh 2

109 St. Mary Street, Cardiff

39 King Street, Manchester 2

50 Fairfax Street, Bristol 1

2 Edmund Street, Birmingham 3

80 Chichester Street, Belfast

or through any bookseller.

Printed in England

S. O. Code No. 91 - 3 - 12 - 21